International Journal of Theoretical and Applied Research (IJTAR)
ISSN: 2812-5878

Homepage: https://ijtar.journals.ekb.eg

Original article

Effects of Bi_2O_3 on Optical Absorption, Ligand Field Parameters and Structural Properties of Co^{2+} ion-doped lithium borate and lithium borosilicate glass systems

AL-Sh.Ramadan[a], Sh.Neseem[a], M. Farouk[b], E.Nabhan[a]

[a]*Physics Department, Faculty of Science, Girls' Branch, Al-Azhar University, Cairo, Egypt.*
[b]*Physics Department, Faculty of Science, Boys' Branch, Al-Azhar University, Cairo, Egypt.*

ARTICLE INFO

Received 05/12/2024
Revised 29/12/2024
Accepted 31/12/2024

Keywords

(NBO)
Urbach energy
Ligand field theory
FT-IR

ABSTRACT

In the present study, the impact of bismuth cations on the constructional and optical characters of borate and borosilicate glasses containing CO (hybrid shaped glasses) was studied. Various glass specimens which have divergent quantities of Bi_2O_3 and a fixed quantity of CoO had been synthesized using a melt-quenching method. The physical properties of the synthesized compositions were examined in terms of density (ρ) and molar volume (V_M). The structural properties were investigated using infrared (IR) analysis and optical absorption spectroscopy. FT-IR studies revealed that Bi^{+3} ions cause structural rearrangement by converting tetra-coordinated boron into tri-coordinate boron, thereby increasing the number of non-bridging oxygen atoms (NBO) which, in return, has a noticeable deficiency in the optical band gap energy. The optical band gap energy was reduced; on the other hand Urbach energy grew up. The light absorption transitions of Co^{2+} ions were investigated using ligand field theory.

Graphical abstract

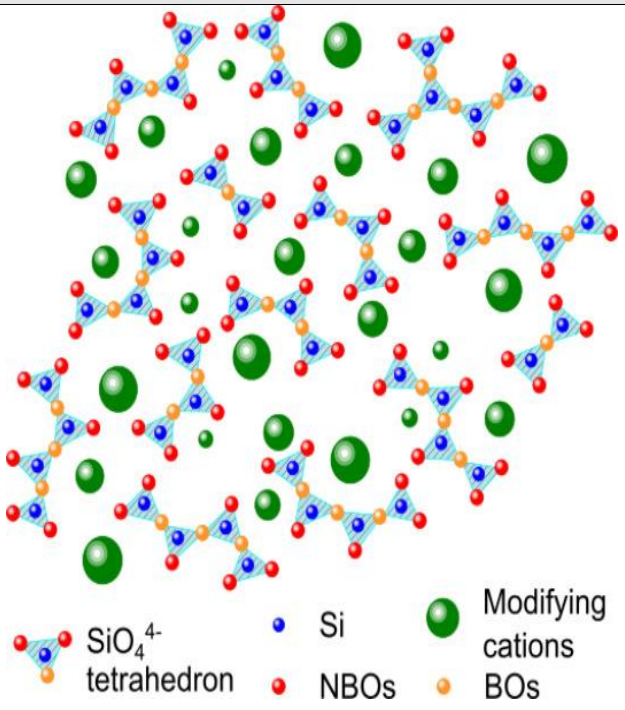

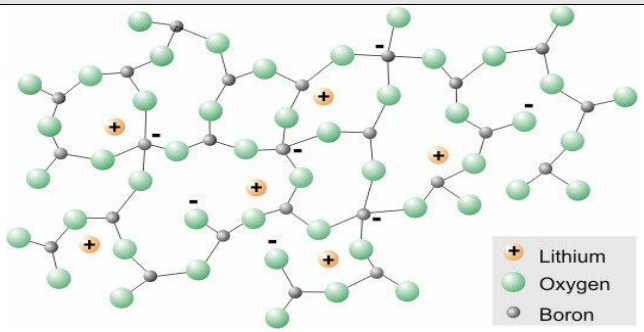

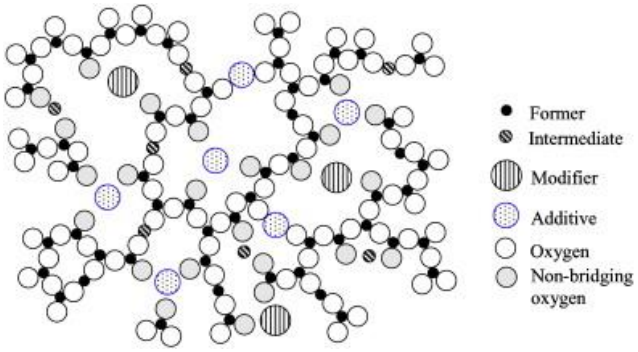

⁎ *Corresponding author*
E-mail address: alshaymaaramadan@yahoo.com
DOI: **10.21608/IJTAR.2024.340662.1096**

1. Introduction

Recently, oxide glasses have captivated the interest of experimenters and scientists because they exhibit important properties that have important uses in numerous applications [1-9]. The selection of an appropriate glass material for a particular application requires information about its various properties [10, 11]. Oxide glasses are traditionally clearly defined as networks composed of components for example SiO_2, B_2O_3, and modifiers like alkaline oxides: Li_2O or metal oxides: Bi_2O_3 [12, 13]. In these glasses, metal oxide oxygen takes part of the covalent glass network and forms extra unfamiliar building blocks. The modifier oxide cations are usually located near the non-bridging oxygen's (NBO) in the glass structure. The extent of network modification clearly relays on the concentration of the modifier oxide exist in the glass. The glass network impacts different physical properties, like density and molar volume.

B_2O_3-based glasses, known as borate glasses, have paid the attention of many investigators because of their important properties, low melting temperatures, thermal stability, and transparency. The most practical uses are in optical, laser, electrical, and photovoltaic devices. Borosilicate glasses with hybrid network formers received great attention during recent years because they combine the stability of silicate glasses with the higher solubility of transition metal ions in borate glasses [14-17]. In addition, transition metal ion (TM) glasses are valuable materials because of their important applications in solid-state lasers, phosphors, optical fibers, memory devices, and photo-conductive devices. (TM) ions are featured by partially filled d- shells that can occur in many oxidation states, where electro-optical conductivity can be generated by the transition of electrons from lower energy levels to higher energy levels. In addition to their beneficial applications in the field of life, they are also used for glass structure identification because their outer d- orbital functions posses a wide radial distribution and high echoes to neighboring cations [18, 19].

Depending on the kind of transition metal ion and other variables, alkali borate and borosilicate glasses containing transition metal ions have vivid colors. Under normal circumstances, cobalt is more stable because it is an anti-ferromagnetic substance [20]. The blue to pink-colored glass is due to the presence of divalent cobalt ions. Co^{2+} ions have distinctive absorption bands in the visible and near-infrared spectral areas and can be found in tetrahedral and octahedral positions within the amorphous network. It has been proposed that cobalt ions be added to the glass network to enhance glass properties for future technological applications, including phosphors, fuel cells, gas sensors, and super capacitors [21, 22].

The most thorough and detailed method for learning more about the surroundings of metal cations in the presence of anions (ligands) is ligand field theory. A group of variables known as ligand field parameters are offered by ligand field theory. This habitat is studied using these parameters. When a metal cation (M) is encompassed by anions (ligands), the anions generate an electrostatic field that changes the energy of the (M) cation's d orbitals. Due to the electrostatic field generated by the ligands, all d -orbitals increase in energy, with the three higher energy orbitals (t_{2g}) rising above the other two lower energy orbitals (e_g). The energy that separates the two orbital groups (t_{2g} and e_g) is named the crystallographic or ligand field splitting (10Dq). B and C represent determination of the inter-electron repulsion between the 3D electrons in the d- shell of the (M) cation (here, the Co^{+2} cation). When TM ions are present in the glass matrix, these properties are readily ascertained. The glass matrix under investigation contained cobalt ions, which led to the computation of the ligand field strength, 10 Dq, and Racah parameters (B and C) based on the energy site of a particular optical transition identified from the optical absorption spectrum [22, 23].

Bi_2O_3 is a transient glass network former due to the high polarizability of this heavy metal ion (Bi^{3+}) and its capacity to reduce its coordination number from VI to III [24]. Therefore, in the existence of glassy network-forming cations, such as, for example, P^{5+}, Si^{4+}, B^{3+}, and Ge^{4+}, a significant structural effect occurs, as it can react as a glass former that introduces pyramidal [BiO_3] units or as a modifier that produces so distorted octahedral [BiO_6] units, relying on the quantity of Bi^{3+} ions present in the glass structure [25, 26]. Bismuth oxide-based glasses are well-defined for their remarkable optical properties and their applications in optical and electronic devices [27, 28].

In this work, we will synthesize lithium bismuth borate and lithium bismuth borosilicate from cobalt oxide and study their structural and optical properties based on ligand field theory.

2. Experimental

Using the conventional melt quenching technique, lithium bismuth borate and lithium bismuth borosilicate glass systems doped with 1% of CoO were prepared. High purity materials of [Li_2CO_3, H_3BO_3, CoO, SiO_2, and Bi_2O_3] were employed as starting materials. Table 1 lists the chemical composition (mol%) of the glass systems with the names BBLC and BBSLC, respectively.

Batches weighing roughly 15 g were completely mixed and ground in an agate mortar before being melted in an electrical muffle furnace in a porcelain crucible until reaching 1100°C. The temperature was maintained at this level for about 90 minutes to allow the melt to be completely homogenous and acquire the desired viscosity. More uniformity was confirmed by repeatedly swirling the molten substance. After that, the free-bubble melts were rapidly cooled (quenched) at room temperature by being poured between two copper plates that had been heated beforehand (poured on a copper plate and another copper plate was put on the first one, i.e., sandwiching) to obtain thin disk-shaped glass samples with smooth and flat surfaces for characterization. The residual parts of the glasses were crushed into fine powder for FT-IR spectral exploration and optical investigations. The use of Pt crucibles and low melting temperatures are important features.

Table (1) the chemical composition (in mol %) details of glass systems.

Sample No.	**((59-x)B_2O_3-xBi_2O_3-40Li_2O-1CoO)**				
BBLC0	59B_2O_3	0 Bi_2O_3	0SiO_2	40Li_2O	1CoO
BBLC 5	54B_2O_3	5 Bi_2O_3	0SiO_2	40Li_2O	1CoO
BBLC 10	49B_2O_3	10 Bi_2O_3	0SiO_2	40Li_2O	1CoO
BBLC 20	39B_2O_3	20 Bi_2O_3	0SiO_2	40Li_2O	1CoO
	((49-x)B_2O_3-xBi_2O_3-10SiO_2-40Li_2O-1CoO)				
BBSLC0	49B_2O_3	0Bi_2O_3	10SiO_2	40Li_2O	1CoO
BBSLC5	44B_2O_3	5Bi_2O_3	10SiO_2	40Li_2O	1CoO
BBSLC10	39B_2O_3	10Bi_2O_3	10SiO_2	40Li_2O	1CoO
BBSLC20	29B_2O_3	20Bi_2O_3	10SiO_2	40Li_2O	1CoO

Using the KBr pellet approach, the FT-IR Nicolet (iS50 spectrometer) from Thermo Fisher Scientific was used to measure the FT-IR absorption spectra of all samples in the (400-4000 cm^{-1}) range at room temperature (RT= 300 K), KBr ratio was 197mg to 3mg of the glass sample (this for all samples).

In the wavelength range of (200–2200 nm), the optical absorption spectra of glasses were determined using a double beam (UV/VIS/NIR) spectrophotometer (type JASCOCrop., V-670, Japan).

3. Results and discussion:

3.1 Density and molar volume

The most basic measurable physical property is the density of a solid. It is also among the precise instruments for differentiating structural differences within the glass network. Any structural alterations to the glass network are reflected in it. Using the Archimedes principal, the produced glasses' density was determined. After weighing each sample in the air, it was placed in room-temperature xylene. The following formula [29] was used to calculate the sample densities:

$$\rho = \frac{Wa}{Wa-Wb} * \rho b \quad (1)$$

Where ρ represents the glass sample's density, W_a denotes its weight in air, W_b denotes its weight in xylene, and ρ_b is xylene's density (assuming xylene has a density of 0.86 g/cm^3). A sensitive single-pan digital electronic balance with an accuracy of (0.0001) g was used for getting the weight of the prepared samples [30].

The density of the BBLC and BBSLC glass systems is shown in Fig. 1. It is evident that when the bismuth content rises successively, so does the sample density. The primary cause of this increase is the substitution of heavier Bi_2O_3 molecules (MW = 465.96 g/mol) for lighter B_2O_3 molecules (MW=69.62g/mol)[28].

Since the molar volume expression shows the spatial distribution of the ions that make up the structure, it is also possible to understand the glass structure there. The preceding structural alterations brought about by a creation or modification process in the glass network are illustrated by the fluctuation in the molar volume with the molar composition of an oxide [14]. It also presents a picture of the glass network's interstitial spacing [31, 32].The molar volume is determined according to the formula:

$$V_M = M/\rho \quad (2)$$

Where M represents the sample's total molecular weight, ρ is its density, and V_M stands for molar volume [33].

As Bi_2O_3 grows in both systems, the molar volume of the glass samples also increases. This can be attributed to the greater bond length radii of Bi_2O_3 (1.03 Å) compared to B_2O_3 (0.273 Å), which causes an increment in free volume in the glass network. Non-bridging oxygen (NBO) production causes the glass structure to become less densely packed and more open as a result [34, 35].

3.2 FT-IR spectroscopy

An essential approach that provides crucial information on the arrangement of the glasses' structural units is FT-IR analysis. For both glass systems, the structural differences in the glass matrix caused by the substitution of Bi_2O_3 for B_2O_3 are explained in figures. (3) and (4). We focus on the mid-IR range (400–1600 cm^{-1}) because the observed glass sample vibration modes are most noticeable. For better clarity, the spectra are shown in this range.

As can be seen, from figures (3)&(4)& table (2) of bands assignment:

Borate glass's infrared spectra are divided into three primary regimes. The first regime is associated with the (B-O-B) bending vibration modes of (BO_3) units and is situated in the (600–800) cm^{-1} range. The B-O bond stretching in (BO_4) units is responsible for the second regime in the range (800–1200) cm^{-1}. The third regime, which vibrates between (1200 and 1600) cm^{-1}, is associated with the B-O stretching in (BO_3) units. Depending on the glass system, these zones occasionally move to higher or lower wave numbers [35–42].

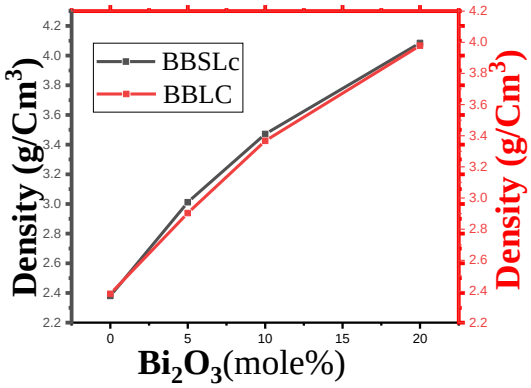

Fig. (1) Variation of density with increase in Bi_2O_3 (in mole %) in prepared samples for both glass systems.

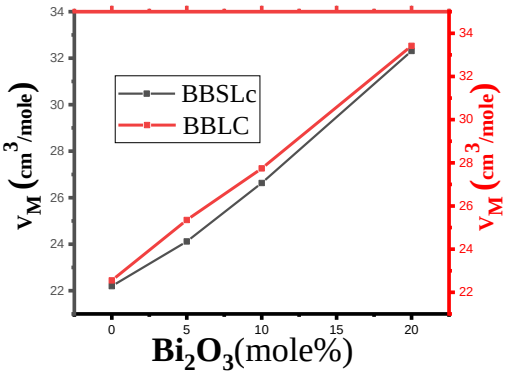

Fig. (2) Variation of molar volume with increase in Bi_2O_3 (in mole %) in prepared samples for both glass systems.

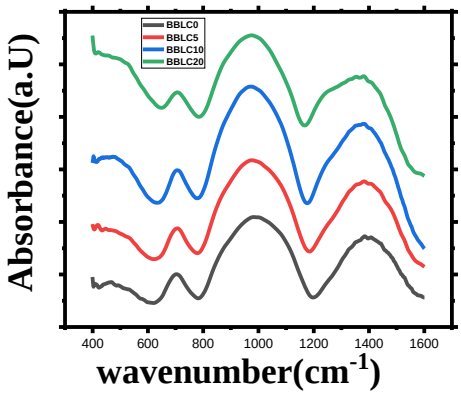

Fig. (3) FTIR spectra of the BBLC glass system.

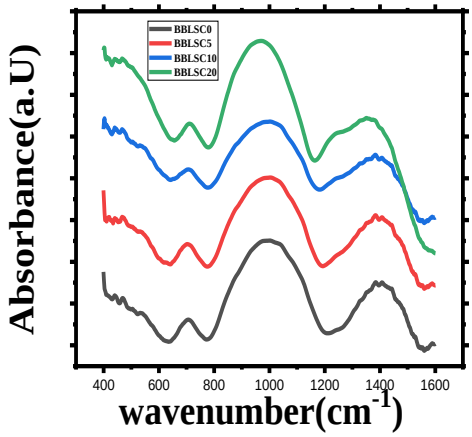

Fig. (4) FTIR spectra of the BBLSC glass system.

Table (2): FT-IR assignment of observed bands of studied glass systems

Band Positions (cm^{-1})	Suggested assignment	References
1300-1500	B-O is stretching vibrations of trigonal BO_3 units.	38-42
800-1200	B-O is stretching vibrations of tetrahedral BO_4 units.	38-41
600-800	Originating from bending vibrations of the borate network (B-O-B)& Si-O-B.	43-45
400-505 and 600	Are generally correlated with Si-O-Si and O-Si-O bending modes.	46-50, 52, 57, 58
770-820	Are attributed to Si-O-Si symmetric stretching of bridging oxygen between tetrahedral.	59,53
910	Si-O-Si stretching of non-bridging oxygen atoms.	54,55
970-1095	Are related to Si-O-Si anti- symmetric stretching of non-bridging oxygen within tetrahedral.	60,52
1309 −1363	asymmetric stretching vibrations of Si-O-Si	61,62
454	The Li–O bond vibrations	66-68
522	Is allocated to Co^{3+} -O bond vibrations.	21,22
485	Bending modes of B-O-B & or Bi–O bands vibrations in (BiO_6).	57,58,50-52
635 – 704	Bi –O bond symmetric stretching vibrations in [BiO_3] units	59 , 57 , 52
850	Vibrations of [BiO_6] octahedral.	52, 63,64
1289	Bi- O−non bridging oxygens (NBOs) in pyramidal [BiO_3] units.	42,56,65

In the glass system BBLC for x = (0, 5, 10, and 20): Only at x = 0, there is a peak at (468) cm^{-1} assigned to Li-bending vibrations (Li-O-Li) due to the absence of Bi_2O_3 [63- 65].

- As we add Bi_2O_3, this peak becomes broader owing to the existence of Bi-O band vibrations in (BiO_6) [47, 49, 54, 55].
- At (x=0) there is a sharp peak at (703) cm^{-1}attributed to bending vibrations of the borate network (B-O-B), and as B_2O_3 is replaced by Bi_2O_3, this peak increases (it belongs to Bi-O bond symmetric vibration in [BiO_3] units) till (x=10) mol%, and at (x=20) mol% the intensity of this peak decreases [49, 54, 55].

- At (800-1200) cm^{-1} there is a large band owing to (B-O) stretching vibrations of tetrahedral BO_4 units [35-39]. And as Bi_2O_3 is added at (x = 5), this band becomes slightly sharp and slightly increases in intensity due to the existence of vibrations of BiO_6 octahedral [49, 60, 61] and at (x = 10), the intensity of this band largely increases and the width of the band decreases. At (x = 20), the band becomes more broad.
- There is a shoulder that appears at about (1250) cm^{-1} from (x = 5), which is related to (Bi-O) non-bridging oxygen in pyramidal (BiO_3) units [39, 53, 62].
- At (1330-1500) cm^{-1} there is a broad band attributed to BO_3 stretching vibrations of triagonal BO_3 [35-39].

In the second glass system (mixed former BBLSC for x = 0, 5, 10, and 20) after doping SiO_2, there are a notable alterations in intensity and band position that happen for all those vibrational modes.

- The band observed below (500) cm^{-1} which belongs to the modifier, gains intensity after doping SiO_2 resulting from (Si-O-Si) and (O-Si-O) bending modes of bridging oxygen`s [43-46, 47-49, 54, 55].
- The BO_4 band region becomes broader because of the formation of (Si-O-Si) and (B-O-Si) [40-42].
- Likewise, the BO_3 band region becomes broader because of the existence of asymmetric stretching vibrations of Si-O-Si [58, 59].
- At (1280) cm^{-1}, there is a small shoulder that belongs to Bi-O non-bridging oxygen (NBOs) in pyramidal (BiO_3) units [39, 53, 62].

It is evident from the explanation above that broad bands exist in many glasses, possibly as a result of distinct neighboring peaks overlapping. The IR spectra of each glass sample was deconvoluted into distinct peaks using the Gaussian distribution function and the curve fit feature of Origin Pro 8.6 software to determine the precise peak position of each band.

As an example figure, the deconvoluted FTIR spectrum of a glass sample with x = 10 is shown in Figs. (5) & (6) for both glass systems. The glass specimen has many peaks, each identified by unique characteristic features such as peak center (x_c), relative area (A), and full width at half maximum (w). Similarly, the residual compositions show the same behavior. The relative area of each peak and its peak center indicate the presence of a specified structural group concentration in the glass matrix and a unique kind of vibration, respectively. For both glass systems, BBLC and BBLSC, the proportion of four coordination boron atoms was calculated using deconvolution data and formula (3) [66, 67]:

$$N_4=A_4/(A_4+A_3) \quad (3)$$

Where A_4 and A_3 are the areas under the peaks of BO4 and BO3, respectively.

Because of the conversion of BO_4 to BO_3, the N_4 values decreased as the Bi_2O_3 content grew as indicated in fig.7. This suggests that an NBO formation process was occurring as bismuth oxide was added to the network, making a loose glass network in both systems. This is the intended outcome for the work's purpose. In comparison to bismuth borate, the open network performs better in the bismuth borosilicate system (in the mixed former network).

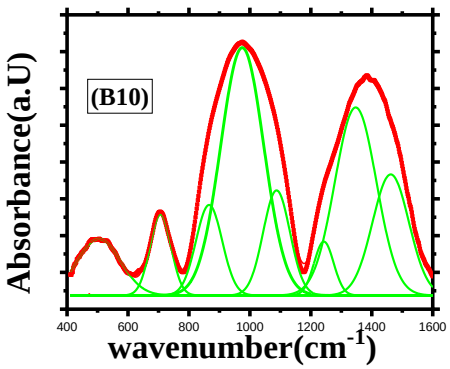

Fig. (5) The deconvoluted IR spectrum of the sample that contains ((49)B_2O_3-10Bi_2O_3-40Li_2O-1CoO) as a representative figure.

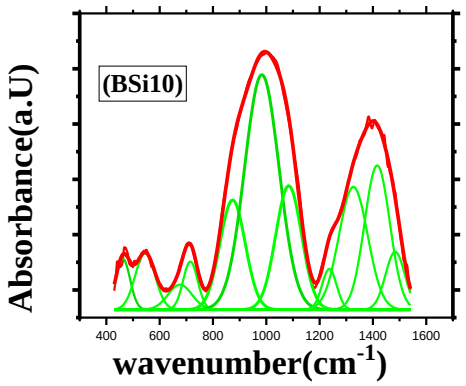

Fig. (6) The deconvoluted IR spectrum of the sample that contains ((39)B_2O_3-10Bi_2O_3-10SiO_2-40Li_2O-1CoO)as a representative figure.

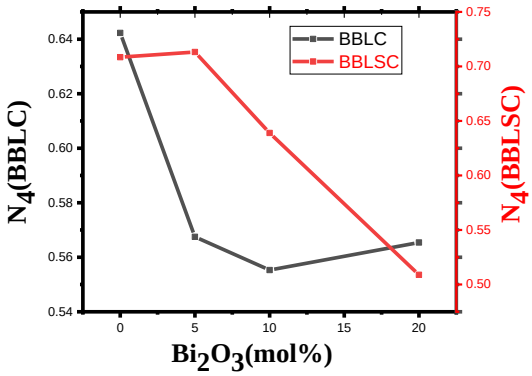

Fig. (7) Variation of N_4 ratio vs. Bi_2O_3 content for both glass systems

3.3 Optical studies

UV-Visible absorption spectra

Fundamentally, optical investigation mostly provides information about the band structure of the glass and other related parameters. For every glass sample that was prepared, the optical absorption spectrum was provided. Fig. 8(a, b) represents a sample that is considered as a

good example. The existence of the glass state in the produced specimens is shown by the absorption spectra's disappearance of a prominent absorption edge [68].Under all conditions, a significant UV absorption is noted, and the absorption edge widens in the visible and near-infrared bands.

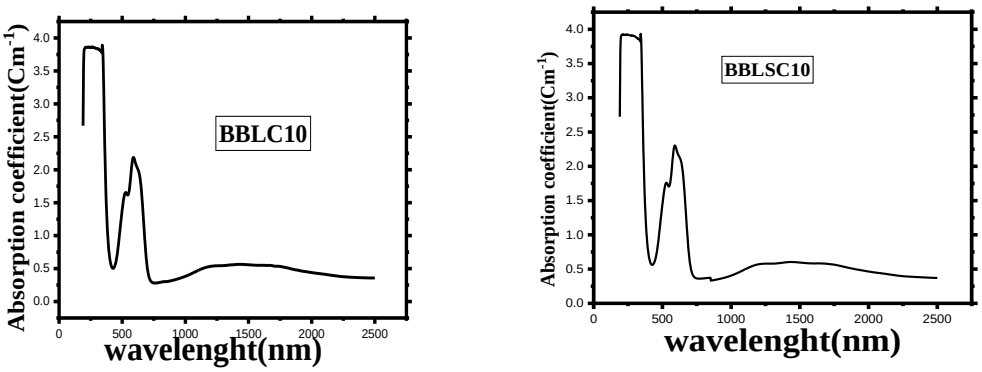

Fig. (8 -a, b)UV- visible spectra for BBLC & BBLSC system.

Optical absorption spectra are utilized to determine Urbach's energy values and the optical band gap. In the electrical band structure of solids, the band gap commonly denotes the variation in energy between the top of the valence band and bottom of the conduction band. The energy desired to release an outer shell electron from its orbit and produce a mobile charge carrier that may move freely within the solid is known as the band gap value, and it is used to determine the material's electrical conductivity. Using formula (4), one may find the absorption coefficient α near the edge of the absorption spectrum:

$$\alpha = \frac{(2.303)A}{t} \quad (4)$$

Where (t) is the thickness of the glass samples and A is absorbance [21].

Mott and Davis theory introduced the relationship between α and photon. Energy hυ indicated in formula (5) [69-71].

$$\alpha \hbar V B(\hbar V - \mathrm{Eg})^b \quad (5)$$

Where hV is the photon energy, B is a constant, $E_g(E_{opt})$ is the optical band energy, b is taken values (2, 1/2, 3, and 2/3) depending on the type of electronic transition, indirect allowed, direct allowed, indirect forbidden, direct forbidden transition respectively.

Electronic structure theory indicated that, indirect allowed transition is the most probable for glassy materials. The values of the optical band gap energy can be estimated from drawing $(\alpha hV)^{1/2}$ vs hV (Tauc's plot), and extrapolating the linear of the curve to $(\alpha hV)^{1/2}=0$ as indicated in Fig. (9-a,b).

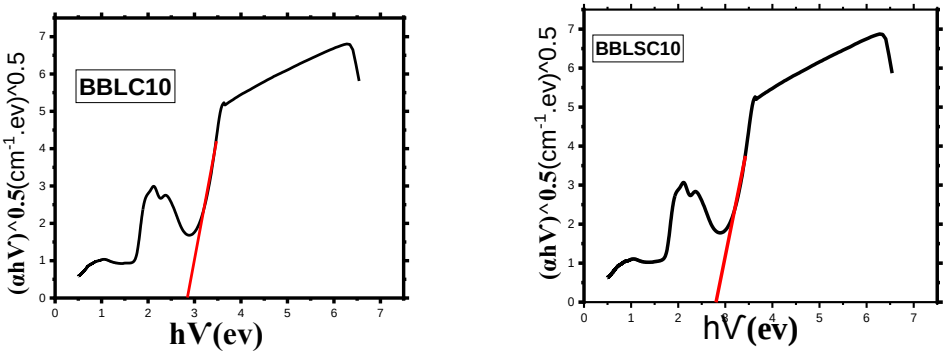

Fig. (9- a, b) Tauc's plots for BBLC& BBLSC system to determine optical band gap values.

It is evident from Fig. (10), that as the concentration of Bi_2O_3 increases, the optical band gap $E_g(E_{opt})$ values decrease. The FT-IR spectra [73], which are associated with the addition of Bi_2O_3, demonstrate that this reduction in E_{opt} can be assigned to the increase of NBOs. Furthermore, NBO ions increase the degree of disorder and are less stable, which results in additional band gap defects [24]. Thus, an increase in NBO ions raises the energy of the valence band, which results in a decrease in optical gap energy.

When the energy of the input photons is less than the optical band gap energy, the region of the absorption spectra is known as the Urbach region. The incident photons in that region are absorbed exponentially, creating an exponential absorption tail known as an Urbach tail in

amorphous materials. One clear indicator of the disorder in the network is the curvature of such a regime. We look up Urbach energy (E_u) to determine the level of disorder in the glass samples. Thus, in these energy gaps, there will be extended or localized states, namely, Urbach energy. The transition from the occupied states of the valence band to the empty tail states of the conduction band results in the scale of band tail width known as Urbach energy [74, 75]. The temperature and static atomic structural disorder determine that energy, or equivalently the band tail width (E_u) [75, 76]. Using the Tauc and Urbach formula (6) [77], this energy is computed:

$$\alpha = \alpha_o \, exp\left(\frac{h\nu}{Eu}\right) \quad (6)$$

Where E_u is Urbach energy and α_0 is a constant. Urbach energy values, acquired from the inverse slope of a linear region of the plot [ln (α) vs. ($h\nu$)] Fig. (11-a,b).

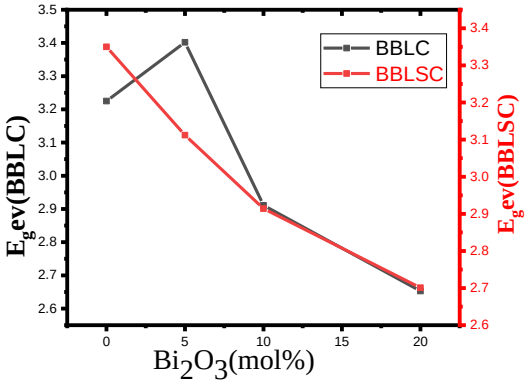

Fig. (10) the optical band gap (E_g) vs. Bi_2O_3 content for both glass systems.

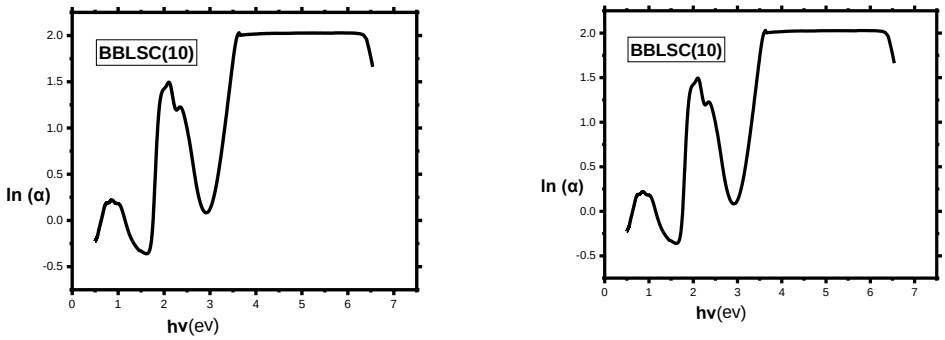

Fig. (11-a,b) Urbach's Plot r for *x*=10 (mol %) in BBLC& BBLSC glass systems.

Table (3) Optical band gap energy (E_g) & Urbach energy (E_u) of BBLC&BBLSC glass systems.

Sample mole%	E_g(ev)	E_u(ev)
BBLC0	3.225	0.341
BBLC5	3.402	0.375
BBLC10	2.911	0.401
BBLC20	2.653	0.502

Sample mole%	E_g(ev)	E_u(ev)
BBLSC0	3.350	0.322
BBLSC5	3.112	0.338
BBLSC10	2.914	0.405
BBLSC20	2.701	0.418

The increase in E_u levels is most likely caused by an increase in disorder degree during the production of NBO and bond relaxing. Moreover, the rise in E_u values indicates a decline in the stability of the structure because of glass matrix fault formation [78]. As a result, the band gap energy drops and the rise in E_u are consistent.

Based on the anticipated band positions of (v_2 and v_3) fig(12-a,b) the predicted crystal field parameter [10Dq] and Racah parameters [B & C] were determined. The energy levels of Co^{2+} (d^7) ions in the tetrahedral field are separated into crystal fields by 10Dq, which is just the (d^3) electronic configuration in the octahedral field [79]. The TM ions Co^{2+} exhibit coulomb repulsion in their d-shell, as indicated by the B & C parameters. These parameters were computed using the formulas [24, 80]as follows:

$$10Dq + 5B = 1/3(V_2 + V_3) \quad (7)$$

$$B = \frac{1}{510}[7(V_2 + V_3) \pm \sqrt{49(V_2 + V_3)^2 + \sqrt{680(V_2 - V_3)^2}}] \quad (8)$$

$$C = 4.63B \pm 0.5 \quad (9)$$

Where v_2 and v_3 are the energy position of optical transitions.

As could be seen in Figure 13(a, b), 10 Dq increased, but when Bi_2O_3 increased, the Racah parameters (B and C) decreased. Increases in 10 Dq values show a significant delocalization of Co^{2+} ion d-electrons, indicating a high level of interaction between these ions and their ligands [81]. The optical band gap was then reduced because of bonding flaws forming in the primary gap. Conversely, the weakening of the field intensity resulting from the repulsion interaction of electrons in the d-shell (i.e., the electrons dispersing over a large distance, reducing the electrostatic interaction) led to the reduction of Racah parameters and the formation of highly covalent bonds between the Co^{2+} ions and their ligands [82, 83]. To guarantee that the inclusion of Bi_2O_3 would enhance the covalency effects on the network bond nature, all of these coefficients were computed.

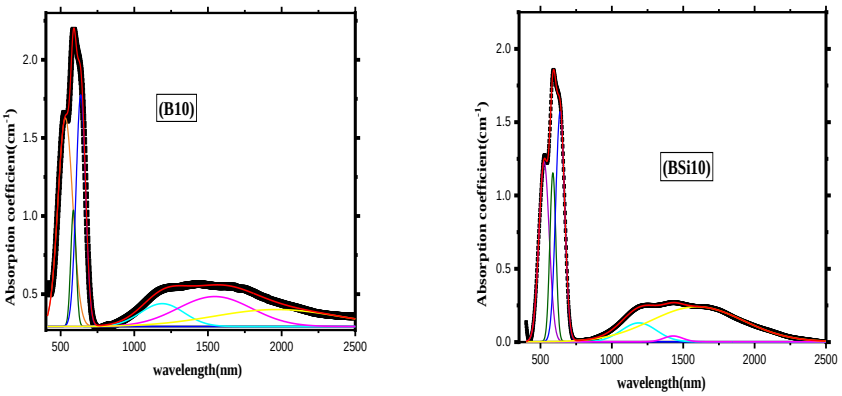

Fig. (12-a, b) Representative deconvoluted optical spectrum for *x*=10 (mol %) in BBLC& BBLSC glass systems.

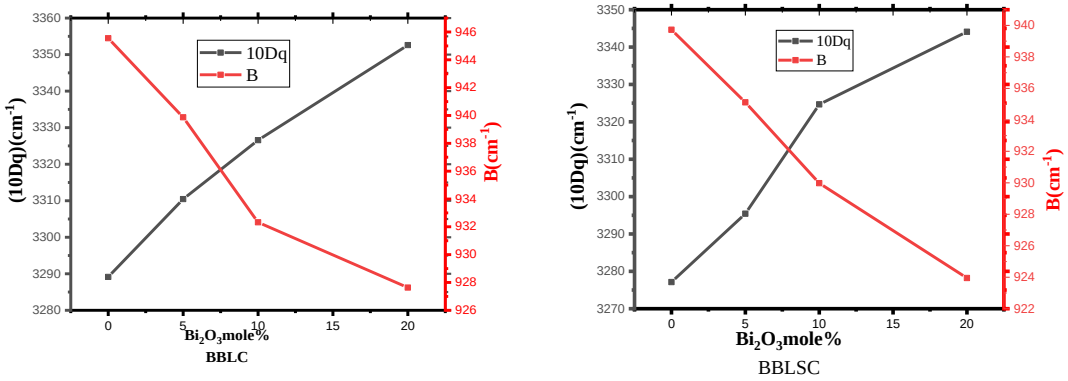

Fig. (13-a,b) The crystal field splitting (10*Dq*) and Racah parameter (*B*) as a function of Bi_2O_3 content for BBLC& BBLSC glass systems.

Table (4): Ligand field strength (10 *Dq*), Racah parameters (*B* and *C*)of BBLC& BBLSC glass systems.

Sample mole%	10 *Dq* (cm^{-1})	B(cm^{-1})	C(cm^{-1})
BBLC0	3289.144	945.5541	4377.916
BBLC5	3310.449	939.8677	4351.587
BBLC10	3326.566	932.3248	4316.664
BBLC20	3352.603	927.6331	4294.941
BBLSC0	3277.115	939.7248	4350.926
BBLSC5	3295.428	935.1105	4329.561
BBLSC10	3324.673	929.9767	4305.792
BBLSC20	3344.1	923.9501	4277.889

4. Conclusion

Using the melt-quenching approach, co-ions-doped bismuth borate and borosilicate glass samples were successfully produced. The characteristics of the glasses under study were impacted by the methodical replacement of B_2O_3 with Bi_2O_3. By using density, FT-IR, and optical absorption, the structure was examined. The decrease in the calculation of N_4 ratios indicated the transformation from BO_4 to BO_3 units based on FT-IR analysis and this leads to the increase in (NBO) ratio. An increase in Urbach energy (eV) correlates with a decrease in band gap (eV), highlighting the significance of Bi_2O_3 in modifying the band gap and its localized states.

Deconvolution and optical spectrum focusing were performed on the cobalt characteristic bands in order to provide additional insight into the d-level splitting and crystal field interaction. The lower binding strength of CoO was identified as the cause of the observed decrease in the optical gap energy. The borosilicate system has less disorder than the borate system, as indicated by the lower values of E_u in the borosilicate system. Therefore, ion mobility is more open in an open matrix than in a borate system.

References

1. R. Rajaramakrishna, Y. Ruangtaweep, N. Sangwaranatee, J. Kaewkhao, J. Non Cryst. Solids 521, 119522(2019). https://doi.org/10.1016/j.jnoncrysol.2019.119522
2. R. Rajaramakrishna, S. Karuthedath, R.V. Anavekar, H. Jain, J. Non Cryst. Solids 358 , 1667–1672(2012). https://doi.org/10.1016/j.jnoncrysol.2012.04.031
3. A. AbdEl_Moneim, Quantitative analysis of elastic moduli and structure of B_2O_3–SiO_2 and Na_2O–B_2O_3–SiO_2 glasses, Phys. B 325, 319–332(2003). https://doi.org/10.1016/S0921-4526(02)01545-4
4. C.A. Maynell, G.A. Saunders, S. Scholes, Ultrasound propagation in glasses in the metastable immiscibility

region of the sodium borosilicate system, J. Non Cryst. Solids 12, 271–294(1973). https://doi.org/10.1016/0022-3093(73)90001-X

5. C. Mercier, G. Palavit, L. Montagne, C. Follet, A survey of transition-metal-containing phosphate glasses, Sci. Paris 5 ,693(2003). https://doi.org/10.1016/S1631-0748%2802%2901437-6
6. G. Tricot, L. Montagne, L. Delevoye, G. Palavit, V. Kostoj, Redox and structure of sodium-vanadophosphate glasses, J. Non Cryst. Solids 345, 56–60(2004). https://doi.org/10.1016/j.jnoncrysol.2004.07.043
7. M.E. Lines, J.B. Macchesney, K.B. Lyons, A.J. Bruce, A.E. Miller, K. Nassau, Calcium aluminate glasses as potential ultralow-loss optical-materials at 1.5–1.9 μm, J. Non Cryst. Solids 107 (2–3) 251–260(1989). https://doi.org/10.1016/0022-3093(89)90470-5
8. F.T. Wallenberger, S.D. Brown, High-modulus glass-fibers for new transportation and infrastructure composites and new infrared uses, Compos. Sci. Technol. 51 (2) 243–263(1994). https://doi.org/10.1016/0266-3538(94)90194-5
9. N.J. Kreidl, Recent applications of glass science, J. Non Cryst. Solids 123, 377–384(1990). https://doi.org/10.1016/0022-3093(90)90810-9
10. J.E. Shackelford, Bioceramics: Applications of Ceramic and Glass Materials in Medicine, Trans Tech Publications Ltd., Enfield, N.H., Uetikon-Zurich, Switzerland, (1999). https://doi.org/10.1201/9781482298093
11. T. Abraham, Advanced Glasses and Glass Ceramics: Materials, Processing, New Developments, Applications, and Markets, Business Communications Co., (1996). https://doi.org/10.1080/10667857.1996.11752656
12. C. -H. Lee, K. H. Joo, J. H. Kim, S. G. Woo, H. -J. Sohn, T. Kang, Y. Park and J. Y. Oh.Characterizations of a new lithium ion conducting Li_2O–SeO_2–B_2O_3 glass electrolyte. Solid State Ionics, Vol. 149, pp. 59-65(2002). https://doi.org/10.1016/S0167-2738(02)00137-6
13. F. Muñoz, L. Montagne, L. Delevoye, A. Durán, L. Pascual, S. Cristol and J-F Paul. Phosphate speciation in sodium borosilicate glasses studied by nuclear magnetic resonance. J. Non-Cryst. Solids, Vol. 352, pp. 2958-2968(2006). http://dx.doi.org/10.1016/j.jnoncrysol.2006.04.016
14. L. Singh, V. Thakur, R. Punia, R.S. Kundu, A. Singh, Structural and optical properties of barium titanate modified bismuth borate glasses, Solid State Sci. 37, 64–71(2014). https://doi.org/10.1016/j.solidstatesciences.2014.08.010
15. M.S. Sadeq, H.Y. Morshidy, Effect of samarium oxide on structural, optical and electrical properties of some alumino-borate glasses with constant copper chloride, J. Rare Earths 38, 770–775(2020). https://doi.org/10.1016/j.jre.2019.11.003
16. S.M. Salem, S.F. Mansour, I.I. Bashter, M.S. Sadeq, A.G. Mostafa, Effect of mixed heavy metal cations on the A.C. conductivity and dielectric properties of some borosilicate glasses, Ceram. Int. 44, 14363–14369(2018). https://doi.org/10.1016/j.ceramint.2020.09.036
17. Thakur, V. Thakur, A. Kaur, L. Singh, Structural, optical and thermal properties of nickel doped bismuth borate glasses, J. Non-Cryst. Solids 512 ,60–71(2019). https://doi.org/10.1016/j.jnoncrysol.2019.02.012
18. Khasa S, Dahiya MS. Structural Investigations of Lithium Vanadoxide,Bismo-Borate Glasses. J IntegrSciTechnol, 1:44–7(2013). https://www.researchgate.net/publication/237076274_Structural_Investigations_of_Lithium_Vanadoxide_Bismo-Borate_Glasses
19. Dalal S, Khasa S, Dahiya MS, Agarwal A, Yadav A, Seth VP, Dahiya S. Effect of substituting iron on structural, thermal and dielectric properties of lithium borate glasses. Mater Res Bull.;70:559–66(2015). http://dx.doi.org/10.1016/j.materresbull.2015.05.017
20. Dalal S, Khasa S, Dahiya MS, Yadav A, Agarwal A, Dahiya S. Optical and thermal investigations on vanadyl doped zinc lithium borate glasses. J Asian Ceram Soc.;3:234–9 (2015). https://doi.org/10.1016/j.jascer.2015.03.004
21. Z.M. Abd El-Fattah, F. Ahmad, M.A. Hassan, Tuning the structural and optical properties in cobalt oxide-doped borosilicate glasses, J. Alloys Compd. 728, 773–779(2017). https://doi.org/10.1016/j.jallcom.2017.09.059
22. M.G. Moustafa, H. Morshidy, A.R. Mohamed, M.M. El-Okr, A comprehensive identification of optical transitions of cobalt ions in lithium borosilicate glasses,J.Non-Cryst.Solids517,9–16(2019). . https://doi.org/10.1016/j. jnoncrysol.2019.04.037
23. S. Sugano, Y. Tanabe, H. Kamimura, Multiplets of transition-metal ions in crystals, Pure Appl. Phys. v. 33 33, xi, 331(1970). https://lib.ugent.be/catalog/rug01:000724156
24 R.G. Burns, Mineralogical Applications of Crystal Field Theory, second ed., Cambridge University, Cambridge, UK , pp,45–86,(1993). https://doi.org/10.1016/j.matpr.2018.08.068
25. M. Farouk, Effect of Co^{2+} ions on the ligand field, optical, and structural properties of ZnLiB glasses, Optik 140 , 186–196(2017). https://doi.org/10.1016/j.ijleo.2017.04.042
26. E.M. Abou Hussein, A.M. Madbouly, F.M. EzzEldin, N.A. ElAlaily, Evaluation of physical and radiation shielding properties of Bi_2O_3–B_2O_3 glass doped transition metals ions, Mater. Chem. Phys. 261, 124212(2021). https://doi.org/10.1016/j.matchemphys.2020.124212
27. Saroj Rani, SujataSanghi, NeetuAhlawat, Ashish Agarwal, Influence of Bi_2O_3 on thermal, structural and dielectric properties of lithium zinc bismuth borate glasses, J. Alloys Compd. 597 110–118,(2014). http://dx.doi.org/10.1016/j.jallcom.2014.01.211
28. D. Saritha, Y. Markandeya, M. Salagram, M. Vithal, A.K. Singh, G. Bhikshamaiah, Effect of Bi_2O_3 on physical, optical and structural studies of ZnO –

Bi_2O_3–B_2O_3, glasses, J. Non. Cryst. Solids 354 (52–54) 5573–5579, (2008). http://dx.doi.org/10.1016/j.jnoncrysol.2008.09.017

29. D.B.Thombre[1], M.D. Thombre[2] "International Journal of Engineering Research and Development" Volume 10, Issue 7, PP.09-19(July 2014).
30. U. B. Chanshetti, V. A. Shelke, S. M. Jadhav, S. G. Shankarwar, T. K. Chondhekar, A. G.Shankarwar, V. Sudarsan, M. S. Jogad FACTA UNIVERSITATIS Series: Physics, Chemistry and Technology Vol. 9, No 1, pp. 29 – 36(2011). Doi:10.2298/FUPCT1101029C
31. J.E.Shelby, Introduction to glass science and technology (the royal society of chemistry, UK, 1997).T.Yano, N.Kunimine, S.Shibata, M.Yamane, J.Non-Cryst.solids 321, p-157(2003). https://doi.org/10.1016/j.jnoncrysol.2023.122664
32. P. Vasantharani and N. Sangeetha. International Journal of Research in Pure and Applied Physics.; 3(1): 1-6(2013). http://dx.doi.org/10.35940/ijitee.A4268.119119
33. A. Wagh, Y. Raviprakash, V. Upadhyaya, S.D. Kamath, Composition dependent structural and optical properties of PbF_2-TeO_2-B_2O_3-Eu_2O_3 glasses, Spectrochim. Acta - Part A Mol. Biomol. Spectrosc. 151, 696–706(2015). https://doi.org/10.1016/j.saa.2015.07.016
34. M. Mariyappan, K. Marimuthu, M.I. Sayyed, M.G. Dong, U. Kara, Effect Bi_2O_3 on the physical, structural and radiation shielding properties of Er^{3+}ions doped bismuth sodium fluoroborate glasses, J. Non. Cryst. Solids 499 (May) 75–85(2018). http://dx.doi.org/10.1016/j.jnoncrysol.2018.07.025
35. AbuoshamaAA,El-Batal FH structural analysis of glassy lead borate containing MoO_3 in relation to its optical properties.Eygpt J solid 29,49-67(2006). Doi:10.21608/EJS.2006.149140
36. El-kheshenAA,El-BatalFH,MarzoukSY,Uv-visible,infrared and Raman spectroscopic and thermal studies of tungsten doped lead borate glasses and the effect of ionizing gamma irradiation .indian J pre apply phys46,225-38(2008).
37. F.H. Abd El-kader, N.A. Hakeem, W.H. Osman, A.A. Menazea, A.M. Abdelghany, Nanosecond laser irradiation as new route for silver nanoparticles precipitation in glassy matrix. SILICON **11**(1), 377–381 (2019). https://doi.org/10.1007/s12633-018-9890-4
38. G. El-Damrawi, A.M. Hassan, R. Ramadan, S. El-Jadal, Nuclear magnetic resonance and FTIR structural studies on borosilicateglasses containing iron oxide. New J. Glass Ceram. **6**(04), 47(2016). http://dx.doi.org/10.4236/njgc.2016.64006
39. L. Xia, L. Wang, Q. Xiao, et al., Preparation and luminescence properties of Eu^{3+}-doped calcium bismuth borate red-light-emitting glasses for WLEDs, Journal ofNon-Crystalline Solids 476, 151–157(2017). http://dx.doi.org/10.1016/j.jnoncrysol.2017.09.049
40. Ramadevudu G, Lakshmi Srinivasa Rao S, Shareeffuddin Md, Narasimha Chary M, LakshmipathiRaoM FTIR and optical absorption studies of new magnesium lead borate glasses. Global J Sci Frontier Res Phys Space Sci 12, 41–6(2012).
41. Kamitsos EI, Patsis AP, Karakassides MA, Chryssikos GD Infrared reflectance spectra of lithium borate glasses. J Non Cryst Solid 126, 52–67(1990). https://doi.org/10.1016/0022-3093(90)91023-K
42. A. Yadav, M.S. Dahiya, A. Hooda, C.S. PremKhasa, Structural influence of mixed transition metal ions on lithium bismuth borate glasses. Solid State Sci. **70**, 54–65 (2017). https://doi:10.1016/j.solidstatesciences.2017.06.011
43. A.A. Akatov, B.S. Nikonov, B.I. Omel'yanenko, S.V. Stefanovsky, J.C. Marra, Structure of borosilicate glassy materials with high concentrations of sodium,iron, and aluminum oxides, Glass Phys. Chem. 35 ,245–259(2009).
44. M. Sundara Rao, Ch. Srinivasa Rao, B.V. Raghavaiah, G. SahayaBaskaran, V.Ravi Kumar, I.V. Kityk, N. Veeraiah, The role of ligand coordination on the spectral features of Yb^{3+} ions in lead aluminumsilicate glasses, J. Mol. Struct.1007 ,185–190. (2012). http://dx.doi.org/10.1007/s00340-013-5502-6
45. R. Laopaiboon, C. Bootjomchai, M. Chanphet, J. Laopaiboon, Elastic properties investigation of gamma-radiated barium lead borosilicate glass using ultrasonic technique, Ann. Nucl. Energy 38, 2333–2337(2011). http://dx.doi.org/10.1016/j.anucene.2011.07.035
46. Y. Jaichueai, C. Bootjomchai, J. Laopaiboon1, R. Laopaiboon, The effect of doping Cu_2O on elastic and structural properties of thermoluminescent glass 90RWG–10Na_2O–xCu_2O, Siam Physics Congress, May 20–22(2015). http://dx.doi.org/10.1016/j.radphyschem.2024.112244
47. N. Ahlawat, A. Agarwal, S. Sanghi, N. Ahlawat, Influence of Ba^{2+} ions on defect concentration in bismuth silicate glasses evidenced by FTIR and UV-visible spectroscopy, Phys. Status Solidi Curr. Top. Solid State Phys. 8 3167–3170(2011). http://dx.doi:10.1002/pssc.201000744
48. I. Ardelean, S. Cora, FT-IR, Raman and UV-VIS spectroscopic studies of copper doped 3Bi_2O_3 •B_2O_3 glass matix, J. Mater. Sci. Mater. Electron. 19, 584–588(2008). http://dx.doi: 10.1007/s10854- 007-9393- 3
49. A.M. Efimov, Quantitative IR spectroscopy: applications to studying glass structure and properties, J. Non. Cryst. Solids. 203 ,1–11(1996). http://dx.doi:10.1016/ 0 022-3093(96)0 0327-4
50. M.L. Krishnan, V.V.R.K. Kumar, Photoluminescence properties of LiF bismuth silicate glass, AIP Conf. Proc. 1942. 10.1063/1.5028831(2018). DOI: 10.21608/EJCHEM.2021.103672.4799
51. M.S. Dahiya, A.ShankarMeenakshi, A. Agarwal, S. Khasa, On the role of ZnO on properties of vitreous bismuth silicates, J. Alloys Compd. 696, 688–696(2017).http://dx.doi:10.1016/j.jallcom.2016.11.285
52. M. Dult, R.S. Kundu, N. Berwal, R. Punia, N. Kishore, Manganese modified structural and optical properties of bismuth silicate glasses, J. Mol. Struct. 1089 ,32–37(2015). http://dx.doi: 10.1016/j.molstruc.2015.02.025 .

53. F. He, Z. He, J. Xie, Y. Li, IR and Raman spectra properties of Bi_2O_3-ZnO-B_2O_3- BaO quaternary glass system, Am. J. Anal. Chem. 05 ,1142–1150(2014). http://dx.doi: 10. 4236/ajac.2014.516121
54. N. Berwal, S. Dhankhar, P. Sharma, R.S. Kundu, R. Punia, N. Kishore, Physi- cal, structural and optical characterization of silicate modified bismuth-borate-tellurite glasses, J. Mol. Struct. 1127, 636–644(2017). http://dx.doi: 10.1016/j.molstruc. 2016.08.03
55. R.S. Kundu, M. Dult, R. Punia, R. Parmar, N. Kishore, Titanium induced structural modifications in bismuth silicate glasses, J. Mol. Struct. 1063 ,77–82(2014). http://dx.doi: 10.1016/j.molstruc.2014.01.057
56. O. Rico-Fuentes, E. Sánchez-Aguilera, C. Velasquez, R. Ortega-Alvarado, J.C. Alonso, A. Ortiz, Characterization of spray deposited bismuth oxide thin films and their thermal conversion to bismuth silicate, Thin Solid Films 478,96–102 (2005). http://dx.doi: 10.1016/j.tsf.2004.10.013.
57. F.H. El Batal, Gamma ray interaction with bismuth silicate glasses, Nucl. In- strum. Methods Phys. Res. Sect. B Beam Interact. Mater. Atoms. 254 ,243–253(2007).http://dx.doi:10.1016/j.nimb.2006.11.043 .
58. MrinmoyGarai, BasudebKarmakar, Shibayan Roy, Cr^{+6} Controlled nucleation in Si-o-si asymmetric(SiO_2-MgO-Al_2O_3-K_2O-B_2O_3-F) glass sealant (SOFC), Front. Mater. 31 (2020). http://dx.doi.org/10.3389/fmats.2020.00057.
59. H.A. Saudi, H.M. Gomaa, M.I. Sayyed, I.V. Kityk, Investigation of bismuth sil- icate glass system modified by vanadium and copper cations for structural and gamma-ray shielding properties, SN Appl. Sci. 1 ,1–9(2019). http://dx.doi: 10.1007/ s42452- 019-0197- x .
60. E.M. Abou Hussein, Vitrified municipal waste for the immobilization of radioactive waste: preparation and characterization of borosilicate glasses modified with metal oxides, Silicon 11 (6) 2675–2688(2019). https://link.springer.com/article/10.1007/s12633-018-0056-1
61. H.A. El Batal, E.M. Abou Hussein, N.A. El Alaily, F.M. EzzEldin, Effect of different 3d transition metal oxides on some physical properties of γ-Irradiated Bi_2O_3-B_2O_3 glasses: a comparative study, J. Non-Cryst. Solids 528, 119733(2020). http://dx.doi.org/10.1016/j.jnoncrysol.2019.119733
62. M.A. Marzouk, H.A. ElBatal, F.M. EzzElDin, Optical properties and effect of gamma irradiation on bismuth silicate glasses containing SrO, BaO or PbO, Silicon 5, 283–295(2013). http://dx.doi.org/10.1007/s12633-013-9160-4
63. H.Y. Morshidy, M.S. Sadeq, In fluence of cobalt ions on the structure , phonon emission , phonon absorption and ligand fi eld of some sodium borate glasses, J. Non-Cryst. Solids J. 525 , 6(2019). https://doi.org/10.1016/j. jnoncrysol.2019.119666. http://dx.doi.org/10.1016/j.jnoncrysol.2019.119666
64. H.Y. Morshidy, A.R. Mohamed, A.A. Abul-magd, M.A. Hassan, Ascendancy of Cr^{3+} on Cr^{6+} valence state and its effect on borate glass environment through CdO doping, Mater. Chem. Phys. 285, 126128(2022). https://doi.org/10.1016/j. matchem-phys.2022.126128
65. A.A. Abul-Magd, H.Y. Morshidy, A.M. Abdel-Ghany, The role of NiO on the structural and optical properties of sodium zinc borate glasses, Opt. Mater. 109 (2020). https://doi.org/10.1016/j.optmat.2020.110301.
66. Y.B. Saddeek, K.A. Aly, K.S. Shaaban, A.M. Ali, M.A. Sayed, Elastic, optical and structural features of wide range of CdO- Na2B4O7 glasses, Mater. Res. Express 5, 65204(2018). https://doi.org/10.1088/2053-1591/aac93f.
67. H.Y. Morshidy, M.S. Sadeq, A.R. Mohamed, M.M. El-Okr, The role of $CuCl_2$ in tuning the physical, structural and optical properties of some Al_2O_3–B_2O_3 glasses, J. Non-Cryst. Solids 528 ,28–29(2020). https://doi.org/10.1016/j. jnoncrysol.2019.119749. http://dx.doi.org/10.1016/j.jnoncrysol.2019.119749
68. S. Kaewjaeng, J. Kaewkhao, P. Limsuwan, U. Maghanemi, Effect of BaO on Optical, Physical and Radiation Shielding, ProcediaEng 32 1080–1086(2012). http://dx.doi.org/10.1016/j.proeng.2012.02.058
69. K. Maheshvaran, K. Marimuthu, Concentration dependent Eu^{3+} doped boro-tellurite glasses - Structural and optical investigations, J. Lumin. 132 (9) 2259–2267(2012). http://dx.doi.org/10.1016/j.jlumin.2012.04.022
70. M.G. Moustafa, M.Y. Hassaan, Optical and dielectric properties of transparent, ZrO_2–TiO_2–Li_2B4O_7 glass system, J. Alloys Compd. 710 312–322(2017). http://dx.doi.org/10.1016%2Fj.jallcom.2017.03.192
[71] J. Tauc, Amorphous and Liquid Semiconductor, Plenum, New York, (1974). http://dx.doi.org/10.1007/978-1-4615-8705-7
72. A.Edukondalu,B.Kavitha,M.A.Samee,S.ar-eem,S.Rahman,K.S.Kumar,Mixed alkali tungsten borate glasses-optical and structural properties,J.Alloys Compd.552,157-165,(2013).
73. Mohamed A. Marzouk, Sherief M. Abo-Naf, Hamdia A. Zayed, Nevien S. Hassan, Photoluminescence and semiconducting behavior of Fe, Co, Ni and Cu implanted in heavy metal oxide glasses, J. Mater. Res. Technol. 5, 226–233(2016). http://dx.doi.org/10.1016/j.jmrt.2015.11.003
74. F. Ahmad, Study the effect of alkali/alkaline earth addition on the environment of borochromate glasses by means of spectroscopic analysis, J. Alloys Compd. 586,605–610(2014). http://dx.doi:10.16/JAllCOM.2013.10.105
75. G. Krishna Kumari, Sk. Muntaz Begum, Ch. Rama Krishna, D.V. Sathish,P.N. Murthy, P.S. Rao, R.V.S.S.N. Ravikumar,Physical and optical properties of $Co2^{+}$, Ni^{2+} doped(20ZnO + xLi_2O + (30 - x)K_2O + 50B_2O_3 ($5 \leq x \leq 25$) glasses: observation of mixed alkali effect, Mater.Res. Bull. 47, 2646–2654(2012). https://doi.org/10.1016/j.materresbull.2012.04.075

76. Manal Abdel-Baki, A.M. Salem, F.A. Abdel-Wahab, FouadElDiasty, Bond character, optical properties and ionic conductivity of $Li_2O/B_2O_3/SiO_2/Al_2O_3$ glass: effect of structural substitution of Li_2O for LiCl, J. Non-Cryst. Solids 354 ,4527–4533(2008).
77. F. Urbach, The long-wavelength edge of photographic sensitivity and of the electronic absorption of solids, Phys. Rev. 92, 1324(1953). https://doi.org/10.1103/PhysRev.92.1324
78. A.A. Abul-Magd, H.Y. Morshidy, A.M. Abdel-Ghany, The role of NiO on the structural and optical properties of sodium zinc borate glasses, Opt. Mater. 109 (2020). https://doi.org/10.1016/j.optmat.2020.110301
79. P. Naresh, G. NagaRaju, Ch. Srinivasa Rao, S.V.G.V.A. Prasad, V. Ravi Kumar,N. Veeraiah, Influence of ligand coordination of cobalt ions on structural properties of $ZnO–ZnF_2–B_2O_3$ glass system by means of spectroscopic studies, Physica B 407, 712–718(2012). https://doi.org/10.1007/s11082-019-1819-7
80. F. Ahmad, E. Hassan Aly, M. Atef, M.M. ElOkr, Study the influence of zinc oxide addition on cobalt doped alkaline earth borate glasses, J. Alloys Compd. 593,250–255 (2014). http://dx.doi.org/10.1016/j.jallcom.2014.01.067
81. A.A. Abul-Magd, H.Y. Morshidy, A.M. Abdel-Ghany, The role of NiO on the structural and optical properties of sodium zinc borate glasses, Opt. Mater. 109 (2020). https://doi.org/10.1016/j.optmat.2020.110301
82. A.M. Othman, Z.M. Abd El-Fattah, M. Farouk, A.M. Moneep, M.A. Hassan, Optical spectroscopy of chromium doped bismuth-lithium borate glasses, J. Non-Cryst. Solids 558, (2021). https://doi.org/10.1016/j.jnoncrysol.2021.120665.
83. D.L. Wood, J. Ferguson, K. Knox, J.F. Dillon, Crystal-field spectra of d3,7 ions. III. Spectrum of Cr^{3+} in various octahedral crystal fields, J. Chem. Phys. ,39 890–898(1963). https://doi.org/10.1063/1.173438